Predicting High-Risk Patients: A Biomechanical-Based Machine Learning Approach for Coronary Vulnerable Plaques Detection

Anna Corti[1], Marco Stefanati[1], Matteo Leccardi[1], Ovidio De Filippo[2], Alessandro Depaoli[2], Pietro Cerveri[1], Francesco Migliavacca[1], Valentina DA Corino[1,3], José F Rodriguez Matas[1], Luca Mainardi[1], Gabriele Dubini[1]

[1]Politecnico di Milano, Milan, Italy
[2]"Città della Salute e della Scienza di Torino" Hospital, University of Turin, Turin, Italy
[3]Centro Cardiologico Monzino IRCCS, Milan, Italy

Abstract

Detecting vulnerable coronary plaques from coronary computed tomography angiography (CCTA) is crucial for preventing cardiac events, yet current methods are suboptimal. Biomechanical indicators as plaque structural stress and strain, though promising, are underutilized in vulnerability machine learning prediction models. Our study proposes a machine learning pipeline to predict vulnerable patients using biomechanical markers from finite element analysis (FEA), while also considering the variability in mechanical properties.

The study involved 40 patients (33 non-vulnerable and 7 vulnerable) who underwent both CCTA and coronary optical coherence tomography. The 3D coronary artery models were segmented from CCTA, and FEA was performed considering average or variable arterial tissues mechanical properties. Plaque structural stresses and strains, along with patient's pressure data, were used to train decision tree classifiers.

Incorporating variability of the mechanical properties enabled improved classification performances (from AUC of 0.95 vs. 0.99, leave-one-out) demonstrating the effectiveness of considering the material parameter uncertainty in model training. This investigation underscores the promise of biomechanical plaque phenotyping for patient stratification.

1. Introduction

Coronary artery disease (CAD) accounts for 8.9 million annual deaths and represents a major cause of vascular morbidity and mortality worldwide [1]. Coronary vulnerable plaques, namely rupture-prone atherosclerotic plaques, are the main responsible for major adverse cardiac events (MACE): their early detection is crucial for preventing MACE [2]. Nowadays, intravascular imaging modalities are the gold standard for vulnerable plaques detection [3], [4], however, coronary computed tomography angiography (CCTA) is commonly adopted as preliminary screening due to its non-invasiveness. Thus, there has been a recently growing interest in finding non-invasive image markers of plaque vulnerability from CCTA. Plaque rupture deals with a biomechanical destabilization, thus depends on a complex interplay between plaque composition, structural features, biological processes and applied stresses. Several studies demonstrated that increased plaque structural stress is a driving mechanism contributing to plaque rupture, suggesting the potential role of plaque structural stress in stratification of patients at risk of MACE [5]-[12]. Nonetheless, biomechanical-based machine learning (ML) models predicting coronary plaque vulnerability are still rare in the literature and accurate patient stratification based on plaque structural stress remains elusive [13].

Our hypothesis is that a comprehensive plaque biomechanical characterization, relying on accurate description of the arterial tissue composition and incorporating the uncertainty of arterial tissue mechanical properties, coupled with ML techniques can provide effective patient stratification. This study proposes a novel biomechanical-based ML pipeline to predict vulnerable patients. It explores the predictive power of plaque stresses and strains obtained from finite element analysis (FEA) as well as the influence of mechanical properties variability on the prediction.

2. Materials and Methods

2.1. Patient dataset

Forty patients who underwent both CCTA and optical coherence tomography (OCT) imaging at the Azienda Ospedaliero-Universitaria "Città della Salute e della

Scienza" of Torino, Italy were included in the study. Coronary arteries presenting at least one vulnerable plaque (defined through OCT examination) were labelled as vulnerable. Moreover, patients presenting at least one vulnerable coronary artery were considered at high risk. Thus, the dataset comprised 40 patients (with 49 arteries and 167 plaques), 7 of which at high risk, presenting with 7 arteries and 28 plaques labelled as vulnerable.

CCTA was performed using a Revolution CT (GE Healthcare, Milwaukee, WI, USA) and OCT image was performed with a CT system (LightLab Imaging Inc/St Jude Medical, Westford, MA, USA). OCT image analysis was performed by two independent investigators and discordance was resolved by consensus.

2.2. Image segmentation and coronary artery models

The 3D coronary artery models were obtained through semi-automatic segmentation from CCTA images using the plaque analysis software QAngioCT Research Edition (Medis Medical Imaging software, Leiden, The Netherlands). Specifically, the stereolithographic files of the lumen and external coronary artery surfaces together with surfaces delimiting medial (or normal wall), fibrous, fibrous fatty, lipid, and calcific tissues, were generated and exported for analysis. The 3D plaque vessel segments were extracted from the coronary artery models according to plaque proximal and distal locations provided by expert radiologists. For each plaque segment, five evenly distributed sections were analyzed.

2.3. Finite element analysis

The 2D vessel cross-sections were generated through an in-house MATLAB software (The MathWorks Inc, Natick, MA, USA). Figure 1A shows a representative cross-section with a detailed view of the triangular FEA mesh. The arterial cross-sections were modelled as composed by five tissues: medial tissue, fibrous tissue, fibrous-fatty tissue, lipid tissue (or necrotic core), and calcifications. To explore the impact of the variability of mechanical properties in the prediction of vulnerable (i.e., high-risk) patients, two scenarios were considered, namely: (i) arterial tissue components modelled as linear isotropic with average mechanical properties (case A) and (ii) arterial tissue components modelled as linear isotropic with variable mechanical properties (case B) [14], [15]. Figure 1B shows the stress-stretch curves, with the corresponding averaged, maximum, minimum, linearized curves (used in the present study) and experimental range. In particular, the minimum, maximum and average Young modulus, E, (Table 1) were computed by fitting the corresponding stress-strain curves up to a 10% strain [14]. Finally, the tissue components were modelled as quasi-incompressible materials, with Poisson's ratio ν=0.475, except for calcifications (ν=0.3) [15].

Simulations were carried out by considering the average mechanical properties for case A, and 200 different combinations of mechanical parameters within the range in Table 1, for case B. Patient-specific dynamic pressure (i.e., difference between the systolic and diastolic pressure) was imposed at the luminal surface, and Robin boundary condition was prescribed at the external surface [16].

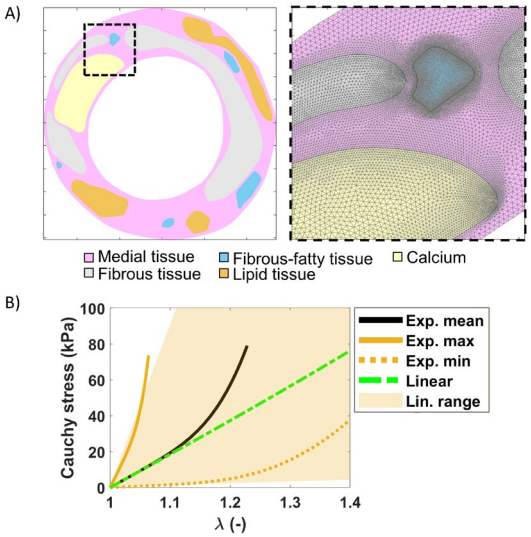

Figure 1. A) Example of coronary artery cross-section with triangular finite element mesh. B) Mechanical properties of lipid tissue.

Table 1. Tissue Young Modulus (E)

Tissue	Min E	Max E	Mean E
Medial tissue	8.9×10^{1}	3.6×10^{3}	7.33×10^{2}
Fibrous tissue	5.8×10^{1}	4.9×10^{3}	8.61×10^{2}
Fibrous-fatty tissue	2.9×10^{1}	2.5×10^{3}	4.31×10^{2}
Lipid core	1.3×10^{1}	9.5×10^{2}	1.89×10^{2}
Calcifications	1.0×10^{7}	2.0×10^{7}	1.5×10^{7}

2.4. Machine learning model development

To develop the ML model for predicting vulnerable patients, the peak von Mises stress and maximum equivalent strain of each plaque were considered, besides the patient's systolic, diastolic and dynamic pressures. For the case A, one peak stress and strain value were computed for each cross-section from FEA, and then averaged over the five cross-sections, to obtain single peak stress and strain value for each plaque. For the case B, 200 values of peak stress and strain were computed for each cross-section (from the 200 FEA simulations with variable material combinations), and two different approaches were considered. The first approach (B1) consisted in obtaining a single peak stress and strain for each plaque, by averaging over the 200 values per cross-section, and then

over the five cross-sections. The second approach (B2), consisted in obtaining 200 instances for each plaque with corresponding peak stress and strain resulting from the average of the values over the five cross-sections. The final feature sets consisted in 167×5 plaques×features for A and B1, and (176×200)×5 plaque instances×features for B2.

A two-steps ML pipeline was implemented to stratify vulnerable from non-vulnerable patients, by considering the decision tree classifier. The first step consisted of a leave-one-out cross-validation at the plaque level, resulting in the computation of the predicted probability of each plaque to be in the vulnerable class. Specifically, first feature Z-score normalization was applied to the training set and the mean and standard deviation were used to normalize features in the validation set. Second, a feature selection process was performed on the training set, by identifying the significantly different features (p-value<0.05) between the vulnerable and non-vulnerable plaques, through Mann-Whitney U test. The first 4 features in ascending p-value order were considered, in case of absence or numerous (>4) significant features. Third, data balancing was applied to the training set, encompassing a random undersampling of the majority class and an oversampling of the minority class using the synthetic minority over-sampling technique (SMOTE) [17]. As a result, 120 balanced samples were obtained for cases A and B1, and 8000 for case B2. Finally, an internal 5-fold cross-validation on the training set was performed to tune the decision tree hyperparameters. The trained model was then applied to the validation plaque for the computation of the vulnerability probability.

For case A and B1 a standard leave-one-out scheme was applied; differently, for case B2, a leave-one-group-out scheme was considered in which, at each iteration (over 167), the validation set comprised the 200 instances of a plaque, and the training set the 33200 instances of the remaining 166 plaques. Consequently, a single vulnerability probability was computed for each plaque in the validation set, as average of the 200 predicted probabilities.

The second step of the pipeline consisted of a leave-one-out cross-validation at the patient level, resulting in the final patient stratification. The plaque with the highest probability of being vulnerable for each patient was considered, representing the worst plaque for the patient. At each iteration of the leave-one-out the optimal probability threshold for the binary classification was estimated on the training set based on the maximum Youden's J value (maximizing the difference between the true positive and the false positive rate). The estimated probability threshold was then applied to classify the patient in the validation set.

3. Results

Table 2 presents the classification performance metrics of the cases A, B1 and B2, while Figure 2 depicts the corresponding confusion matrix and receiving operating characteristic (ROC) curve. Overall, good stratification performances were achieved by all three methods (AUC= 0.95; 0.91 and 0.99, for case A, B1, B2, respectively), and the inclusion of the variability in the material mechanical properties slightly improved the stratification performances. Specifically, compared to case A, case B1, improved the sensitivity, by correctly identifying all the 7 vulnerable patients, while slightly decreased the specificity, resulting in an overall improvement in the balanced accuracy. Differently, case B2, identified 6 out of 7 vulnerable patients, as case A, but correctly identified one more non-vulnerable patient with respect to case A, thus resulting in increased balanced accuracy and AUC.

Table 2. Classification metrics for case A, B1 and B2.

Case	Sensitivity	Specificity	AUC	Bal. Acc
A	0.86	0.91	0.95	0.88
B1	1	0.82	0.91	0.91
B2	0.86	0.94	0.99	0.90

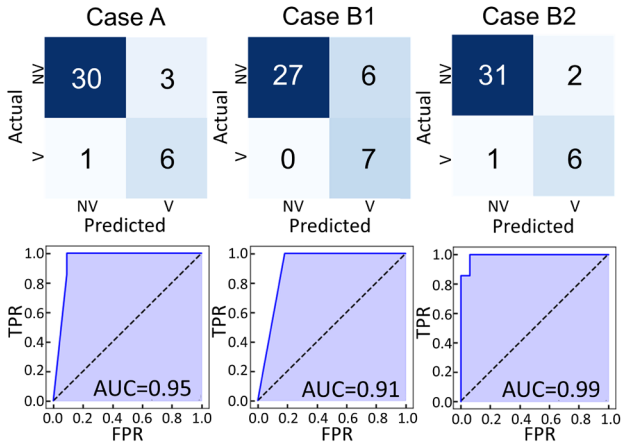

Figure 2. Confusion matrix and receiving operating characteristic (ROC) curve of case A, B1 and B2.

4. Discussion and Conclusions

In the present study, a novel biomechanical-based ML pipeline for stratifying vulnerable patients was proposed. Although the small dataset, high classification performances were obtained, demonstrating the potentiality of the proposed methodology. Moreover, the obtained results suggested that accounting for the variability in arterial tissue material properties has an impact in the model predictive power. In particular, compared to the baseline average case (A), the inclusion of the mechanical variability enabled, in the first case (B1), the identification of all the 7 vulnerable patients (thus maximizing the sensitivity), and in the second case (B2), the achievement of an AUC = 0.99, with only three patients misclassified.

Overall, although biomechanical markers of coronary plaque vulnerability have been proposed, suggesting the peak plaque stress as driving factor [5]-[11], the implementation of biomechanical-driven predictive models is still at early stages. A preliminary study [12] used biomechanical and morphological features to predict the change in a plaque vulnerability index over 10-months, achieving AUC=0.85 on 45 cross-sections of one patient. To the best of the authors' knowledge, our study represents the first biomechanical-based ML approach for the stratification of vulnerable patients, which considers the uncertainty of tissue mechanical properties. This investigation underscores the promise of biomechanical plaque phenotyping, which embeds information on material properties, plaque morphology, and composition, for patient stratification.

Acknowledgments

This work has been partially funded within the Pre-commercial procurement tender by Regione Lombardia – Azienda Socio-Sanitaria Territoriale (ASST) di Pavia, Ref. ASST_2018_PCP01. AC is funded by the National Plan for NRRP Complementary Investments (PNC, established with the decree-law 6 May 2021, n. 59, converted by law n. 101 of 2021) in the call for the funding of research initiatives for technologies and innovative trajectories in the health and care sectors (Directorial Decree n. 931 of 06-06-2022) - project n. PNC0000003 - AdvaNced Technologies for Human-centrEd Medicine (project acronym: ANTHEM). This work reflects only the authors' views and opinions, neither the Ministry for University and Research nor the European Commission can be considered responsible for them. MS is funded by Fondazione Regionale per la Ricerca Biomedica (Regione Lombardia), project 3432721 - AI-CORPS.

References

[1] "Global, regional, and national age-sex-specific mortality for 282 causes of death in 195 countries and territories, 1980-2017: a systematic analysis for the Global Burden of Disease Study 2017.," *Lancet (London, England)*, vol. 392, no. 10159, pp. 1736–1788, Nov. 2018.

[2] P. Gaba, B. J. Gersh, J. Muller, J. Narula, and G. W. Stone, "Evolving concepts of the vulnerable atherosclerotic plaque and the vulnerable patient: implications for patient care and future research.," *Nat. Rev. Cardiol.*, vol. 20, no. 3, pp. 181–196, Mar. 2023.

[3] C. Stefanadis, C.-K. Antoniou, D. Tsiachris, and P. Pietri, "Coronary atherosclerotic vulnerable plaque: current perspectives.," *J. Am. Heart Assoc.*, vol. 6, no. 3, Mar. 2017.

[4] M. J. Bom *et al.*, "Early detection and treatment of the vulnerable coronary plaque: can we prevent acute coronary syndromes?," *Circ. Cardiovasc. Imaging*, vol. 10, no. 5, May 2017.

[5] Z. Teng *et al.*, "Coronary plaque structural stress is associated with plaque composition and subtype and higher in acute coronary syndrome: the BEACON I (Biomechanical Evaluation of Atheromatous Coronary Arteries) study.," *Circ. Cardiovasc. Imaging*, vol. 7, no. 3, pp. 461–470, May 2014.

[6] A. J. Brown *et al.*, "Plaque structural stress estimations improve prediction of future major adverse cardiovascular events after intracoronary imaging.," *Circ. Cardiovasc. Imaging*, vol. 9, no. 6, Jun. 2016.

[7] C. Costopoulos *et al.*, "plaque rupture in coronary atherosclerosis is associated with increased plaque structural stress.," *JACC. Cardiovasc. Imaging*, vol. 10, no. 12, pp. 1472–1483, Dec. 2017.

[8] C. Costopoulos *et al.*, "Heterogeneity of plaque structural stress is increased in plaques leading to MACE: insights from the PROSPECT study.," *JACC. Cardiovasc. Imaging*, vol. 13, no. 5, pp. 1206–1218, May 2020.

[9] S. Z. Gu and M. R. Bennett, "Plaque structural stress: detection, determinants and role in atherosclerotic plaque rupture and progression.," *Front. Cardiovasc. Med.*, vol. 9, p. 875413, 2022.

[10] C. Costopoulos *et al.*, "Impact of combined plaque structural stress and wall shear stress on coronary plaque progression, regression, and changes in composition.," *Eur. Heart J.*, vol. 40, no. 18, pp. 1411–1422, May 2019.

[11] S. Z. Gu *et al.*, "Comprehensive biomechanical and anatomical atherosclerotic plaque metrics predict major adverse cardiovascular events: A new tool for clinical decision making.," *Atherosclerosis*, vol. 390, p. 117449, Jan. 2024.

[12] X. Guo *et al.*, "Predicting plaque vulnerability change using intravascular ultrasound + optical coherence tomography image-based fluid-structure interaction models and machine learning methods with patient follow-up data: a feasibility study.," *Biomed. Eng. Online*, vol. 20, no. 1, p. 34, Apr. 2021.

[13] R. Lv *et al.*, "Image-based biomechanical modeling for coronary atherosclerotic plaque progression and vulnerability prediction.," *Int. J. Cardiol.*, vol. 352, pp. 1–8, Apr. 2022.

[14] Z. Teng *et al.*, "Material properties of components in human carotid atherosclerotic plaques: a uniaxial extension study.," *Acta Biomater.*, vol. 10, no. 12, pp. 5055–5063, Dec. 2014.

[15] M. Stefanati *et al.*, "Effect of variability of mechanical properties on the predictive capabilities of vulnerable coronary plaques.," *Comput. Methods Programs Biomed.*, vol. 254, p. 108271, Jun. 2024.

[16] S. Gahima, P. Díez, M. Stefanati, J. F. Rodriguez Matas, and A. García-González, "An unfitted method with elastic bed boundary conditions for the analysis of heterogeneous arterial sections," *Mathematics*, vol. 11, pp. 1748, 2023.

[17] N. V Chawla, K. W. Bowyer, L. O. Hall, and W. P. Kegelmeyer, "SMOTE: synthetic minority over-sampling technique," *J. Artif. Int. Res.*, vol. 16, no. 1, pp. 321–357, 2002.

Address for correspondence:
Anna Corti.
Department of Electronics, Information and Bioengineering, Politecnico di Milano, Via Ponzio 34/5, 20133 Milan, Italy
anna.corti@polimi.it